

## Low-energy conductivity of PF<sub>6</sub>-doped polypyrrole

B. Chapman

*Industrial Research, P.O. Box 31-310, Lower Hutt, New Zealand  
and School of Chemical and Physical Sciences, Victoria University of Wellington, P.O. Box 600, Wellington, New Zealand*

R. G. Buckley

*Industrial Research, P.O. Box 31-310, Lower Hutt, New Zealand*

N. T. Kemp, A. B. Kaiser, D. Beaglehole, and H. J. Trodahl

*School of Chemical and Physical Sciences, Victoria University of Wellington, P.O. Box 600, Wellington, New Zealand*

(Received 6 July 1999)

In this paper we present a set of temperature-dependent reflectivity and dc conductivity measurements on a series of PF<sub>6</sub>-doped polypyrrole samples differing only in their synthesis temperatures, spanning the metal-insulator transition. From the reflectivity we have derived optical constants, taking particular care that they are Kramers-Kronig consistent. We have analyzed our data in the light of two proposed models for the structure of conducting polymers, homogeneous and inhomogeneous disorder, and find that the observed decrease in the low-energy ac conductivity can be accounted for by a simple generalization of the heterogeneous disorder model used to explain the dc conductivity. The homogeneous localization-modified Drude model fails to satisfactorily model the ac conductivity at low energy. [S0163-1829(99)06043-9]

### I. INTRODUCTION

There is currently considerable interest in the conductivity mechanisms of doped conducting polymers, which has as its focus the relationship between the conductivity and the morphology of the polymer. The conductivities of some polymers are remarkably high; for instance PF<sub>6</sub>-doped polypyrrole can have conductivities in the range of 100–500 (Ω cm)<sup>-1</sup>. While conducting polymers display some metalliclike properties, such as metallic thermopowers, increasing reflectivities for decreasing spectral energies in the infrared and in some cases finite zero temperature conductivities, they also display non-metallic-like properties such as semiconductorlike temperature coefficients of conductivity and anomalous energy-dependent conductivities. Reconciling these seemingly contrasting properties has been a point of debate.<sup>1-7</sup>

The dc conductivity of polypyrrole as a function of preparation conditions, dopant, and temperature has been widely reported and two comprehensive studies of infrared reflectivity measurements on a similar range of samples exist. The similarity between reported results is notable. However, different interpretations exist for the qualitatively similar data. Some describe their data in terms of disorder-induced localization and interpret the polymers as lying near a metal-insulator transition.<sup>2,3</sup> Others interpret their data as providing evidence of a true mix of metalliclike and nonmetallic components.<sup>4-7</sup> A significant difference in the two treatments is in the analysis of the optical constants derived from the reflectivity. Some workers report large negative dielectric constants at low energy and argue for a small fraction of metallic carriers with large mean free paths, the bulk of the carriers being localized due to disorder.<sup>4</sup> Others do not observe a negative dielectric constant at low energies and instead interpret their energy-dependent conductivity as de-

scribing 3-dimensional Anderson localization in a homogeneous material by noting that the data fits a localization-modified Drude model.<sup>3</sup>

In this paper we report energy-dependent reflectivity measurements of high photometric accuracy on a series of PF<sub>6</sub>-doped polypyrrole samples grown at different temperatures including reflectivity measurements at two temperatures on the most conducting sample as well as dc conductivity measurements made on the same samples. We have identified the low-energy region of the dielectric constant spectrum as a source of difficulty and have taken particular care in this region. In generating our optical constants we have used a fit to the reflectivity in conjunction with a Kramers-Kronig transform in order to ensure the spectra are fully Kramers-Kronig consistent at low energies.

### II. EXPERIMENT, RESULTS, AND ANALYSIS

Films of doped polypyrrole were prepared by electrochemical deposition from a solution of propylene carbonate and 1% water containing 0.06 mole per liter of monomeric pyrrole and 0.06 mole per liter hexafluorophosphate. They were grown to a thickness of 80 μm on polished glassy carbon at a constant current density of 0.3 mA/cm<sup>2</sup> and under a nitrogen atmosphere. Films were grown at three different temperatures to produce high, medium, and low conductivity films, labeled HC, MC, and LC in Table I which shows the growth temperatures and dc conductivities of the three samples.

TABLE I. Samples.

Label	T <sub>growth</sub>	σ <sub>300 K</sub> [(Ωcm) <sup>-1</sup> ]
HC	-40 °C	332
MC	0 °C	144
LC	20 °C	76

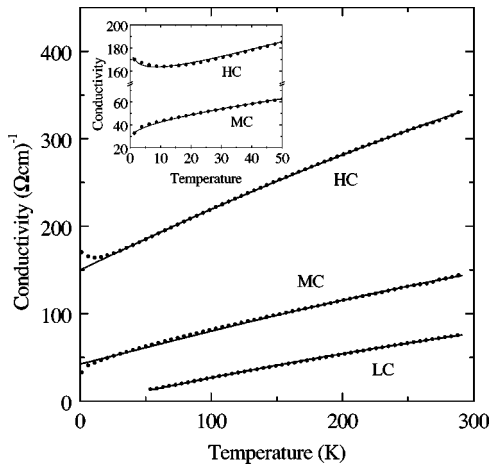


FIG. 1. Temperature-dependent dc conductivities of  $\text{PF}_6$ -doped polypyrrole samples HC, MC, and LC (in descending order). Fluctuation induced hopping fits for the HC and MC samples and the variable range hopping fit for the LC sample are shown as solid lines. The inset shows the fits of the homogeneous model as solid lines to the conductivities of the HC and MC samples for  $T < 50$  K.

The temperature-dependent dc conductivity was measured between 4 K and room temperature with a four-probe technique. The reflectivity measurements were made with a Bomem Fourier transform infrared interferometer (0.0075–1 eV) and a grating spectrometer (0.5–5 eV). The reflected intensity of the sample was compared to the reflected intensity of an evaporated gold film.

The temperature dependence of the dc conductivity of all samples is shown in Fig. 1. The conductivity of all three samples falls from the room temperature value as the temperature is decreased. The HC sample has a minimum near 10 K and a rise at lower temperatures and extrapolates to a finite value at 0 K. The MC sample has a sharp downturn at the lowest temperatures and the LC sample extrapolates to zero conductivity at 0 K.

Measurements comparing the room temperature reflectivity of the samples were made on the highly specular surface of the film that grew against the electrode. The energy-dependent reflectivity [Fig. 2(a)] is composed of structure near 0.1 eV on a broad energy-dependent background. The reflectivity has a minimum at 2 eV and rises at lower energies and is highest and still rising at the lowest measured energy (0.0075 eV).

The energy-dependent conductivity,  $\sigma(\omega) = \sigma_1(\omega) + i\sigma_2(\omega)$ , was extracted in the first instance from the reflectivity with a Kramers-Kronig transform. Extrapolating the reflectivity beyond 5 eV was done using an inverse square dependency to 40 eV and a free electron behavior beyond that.<sup>8</sup> The reflectivity was extrapolated to unity at zero energy using the expression,  $R = 1 - A\omega^x$  [Eq. (1)]. A Hagen-Rubens treatment would set  $x = 0.5$ , appropriate for a purely real and energy-independent conductivity below the measurement region. However, this cannot be used confidently for polypyrrole and hence we have allowed  $x$  to vary about 0.5.

The high reflectivity and extrapolations of this nature mean that the real and imaginary parts of the refractive index,  $n$  and  $k$ , are of similar magnitude. The real part of the

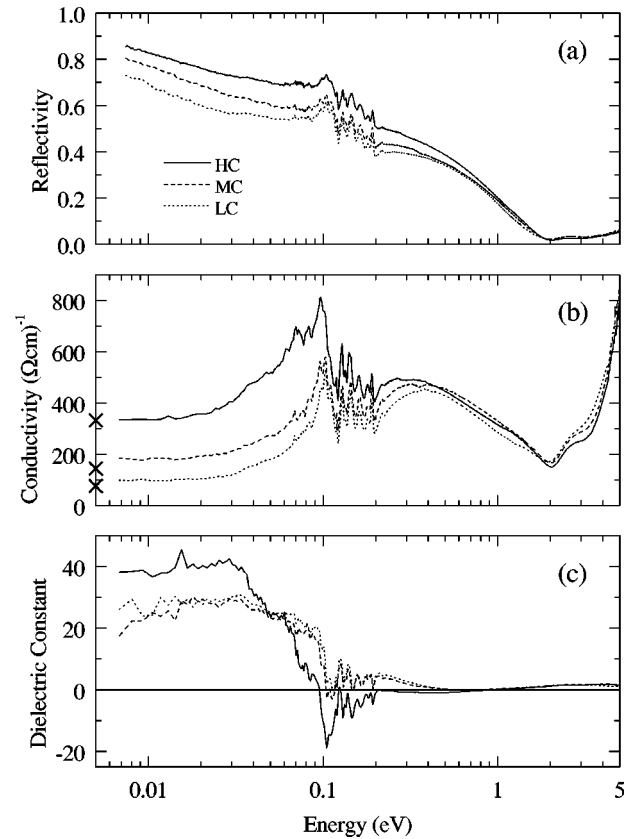


FIG. 2. Reflectivity (a), Kramers-Kronig generated conductivity (b), and dielectric constant (c) of polypyrrole samples HC (solid line), MC (dashed line), and LC (dotted line), displayed on a log energy scale.

dielectric constant  $\epsilon_1(\omega) = 1 - 4\pi\sigma_2(\omega)/\omega$  is related to the complex refractive index by  $\epsilon_1 = n^2 - k^2$ , so that small errors in  $n$  and  $k$  will lead to large errors in  $\epsilon_1$ . We have found that the sign of  $\epsilon_1$  in the range of the low-energy extrapolation is indeed strongly sensitive to the assumed value of  $x$ . The real part of the conductivity, on the other hand, was only weakly dependent on the extrapolation. Note that over the measurement region the results are very much less sensitive to the extrapolation.

As an aid to improving the low-temperature extrapolation we have attempted to reproduce the reflectivity function<sup>9</sup> with a sum of a Drude function  $\sigma(\omega) = \omega_{pD}^2 \tau / 4\pi(1 - i\omega\tau)$ , an oscillator  $\sigma(\omega) = \omega_{pOsc}^2 \omega / 4\pi[i(\omega_0^2 - \omega^2) + \omega\Gamma]$  centered near 0.3 eV, and a number of oscillators to fit the structure near 0.1 eV. The spectrum generated by this model matched the reflectivity extremely closely, particularly below 0.04 eV where the difference between the model and the data was less than 1%, corresponding to the experimental uncertainty in the reflectivity. The optical constants generated were similarly identical to the spectra obtained by the Kramers-Kronig transform *in the measurement region*. By fitting Eq. (1) to the low-energy region of the modeled reflectivity, a best fit value of the exponent,  $x$ , was determined to be 0.48 for the sample HC and used in the Kramers-Kronig transform. In this case a positive low-energy dielectric constant results from the Kramers-Kronig transform while an exponent of 0.5 gives a negative dielectric constant, demonstrating the extreme sensitivity of the sign of the dielectric constant to the

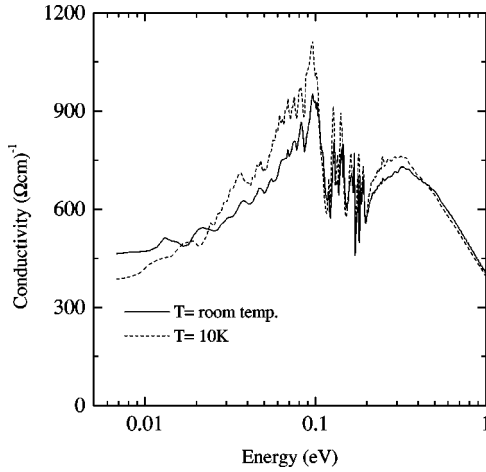


FIG. 3. Conductivity of polypyrrole sample grown at  $-40^{\circ}\text{C}$  measured at room temperature (solid line) and 10 K (dashed line).

magnitude of the exponent and to small changes in the low-energy reflectivity extrapolation. Similar extrapolations were calculated for the MC and LC samples.

The energy-dependent conductivity and dielectric constant over the measured range generated using the Kramers-Kronig transform are shown in Figs. 2(b) and 2(c) for the three samples. The conductivity rises with increasing energy to a series of narrow vibrational peaks and a broad electronic feature near 0.3 eV, which shifts to lower energy in the higher conductivity samples. The low-energy dielectric constant [Fig. 2(c)] is positive and relatively large for all three samples, and the low-energy conductivities are in agreement with the dc conductivities shown by the large crosses on the conductivity axis.

The effect of measurement temperature on the energy-dependent conductivity is shown in Fig. 3. On lowering the temperature from room temperature to 10 K there is a shift in oscillator strength of the midinfrared 0.3 eV peak to lower energies, a growth in oscillator strength of the low-energy peak near 0.1 eV and a decrease in the conductivity at low energy similar to that seen in the dc conductivity. Changes can also be seen in the molecular vibrations; several of the vibrational peaks narrow at the lower temperature and some also soften.

In the dc conductivity we observe a progression through the metal-insulator transition regulated by growth temperature. As the growth temperature decreases the conductivity has a greater magnitude and smaller relative temperature coefficient and extrapolates to a finite conductivity at zero temperature. The energy-dependent conductivity displays a significant shift in oscillator strength to lower energies with decreasing growth temperature. The changes in conductivity have been interpreted<sup>2</sup> as being the result of a change in disorder, the nature and scale of which is undefined. Here we consider two models of the disorder, inhomogeneous and homogeneous disorder, that differ in the scale of disorder, and can account qualitatively for the observed behavior.

#### A. Inhomogeneous disorder

A number of authors have proposed inhomogeneous disordered models to explain dc transport measurements in con-

ducting polymers.<sup>5,7,10</sup> In this case, the charge carriers experience an inhomogeneous environment, with more ordered regions of relatively high, possibly metallic conductivity, interspersed with less ordered regions of lower, possibly insulating conductivity. The conductivity of the polymer then has primarily the temperature dependence of the low conductivity regions but with a magnitude greater than that of the low conductivity component. This inhomogeneous model accounts for the existence of nonmetallic and metallic properties, such as metalliclike thermopower.<sup>5</sup> In this metal/nonmetal composite, the metal-insulator transition is realized by the opening up of percolating paths through the sample. This would come about by an increase in the fractional amount of the metallic component, which would be a natural consequence of a decrease in disorder in the barrier component.

In this inhomogeneous picture, the conductivity can be modeled as a series combination of a “metallic” resistivity,  $\sigma_m^{-1}$ , and a “barrier” resistivity,  $\sigma_b^{-1}$ , so that  $\sigma^{-1} = (g_m \sigma_m)^{-1} + (g_b \sigma_b)^{-1}$ , where  $g_a$  and  $g_b$  are geometrical factors.<sup>6</sup> We have analyzed the dc conductivity of the samples with nonzero extrapolated conductivity at zero temperature using Sheng’s fluctuation induced tunneling model with the form  $\sigma_b(T) = \sigma_t \exp[-T_1/(T+T_0)]$ ,<sup>10</sup> where  $T_0$  and  $T_1$  are constants determined by the height and width of the barrier. The “metallic” resistivity, if it is small in magnitude or only weakly temperature dependent, may produce no obvious effect on the temperature dependence of the total conductivity, but would scale up the magnitude.<sup>6</sup> We have fit this model to the dc conductivity of Fig. 1 and obtain an extremely good fit above 15 K, as shown in Fig. 1. The small anomalies below 15 K are consistent with an additional  $T^{1/2}$  term expected for electron-electron interaction effects in disordered metals, although the sign is anomalous in the HC sample.<sup>11</sup>

We have generalized the two-component model above to take into account energy dependent behavior and generated a form to model the spectral conductivity. The high conductivity, “metallic,” regions are modeled as a Drude conductor,  $\sigma_m(\omega) = \omega_{pD}^2 \tau / 4\pi(1 - i\omega\tau)$ , and the low conductivity, “barrier,” regions as a parallel combination of a resistor of resistivity  $\rho$ , and a capacitor with dielectric constant  $\epsilon_b$ , to give  $\sigma_b(\omega) = \rho^{-1} + i\omega\epsilon_b$ . At low energy the conductivity is dominated by the resistor/capacitor combination and at high energies the capacitor acts as a short circuit and the conductivity is dominated by the Drude component. If the molecular vibrations are ignored then this model describes the main features of the data as illustrated in Fig. 4. In particular, the energy dependence of the low-energy conductivity rises with increasing energy from an intermediate value at zero energy to a peak in the midinfrared before falling away at high energies. The model is also consistent with the observed temperature dependence and growth dependence of the optical conductivity. At higher energies (above 0.025 eV) the metallic component dominates and the observed shift in oscillator strength is due to an increase in the relaxation time  $\tau$  with either decreasing measurement temperature or growth temperature. At lower energies the conductivity is dominated by fluctuation-induced tunneling, which is thermally activated, hence the reduction in conductivity with decreasing measurement temperature or increasing growth temperature.

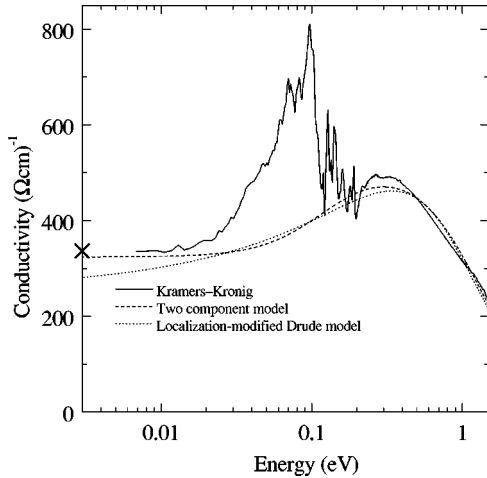


FIG. 4. Fits to the energy-dependent conductivity of the HC sample compared to the Kramers-Kronig transform (solid line). The two-component model (dashed line) and the localization-modified Drude model (dotted line) are shown.

### B. Homogeneous disorder

In homogeneously disordered metals a mobility edge in the density of states separates states localized by disorder from delocalized states.<sup>12</sup> If the Fermi energy lies in the region of localized states the material is insulating and the conductivity at zero temperature is zero. If the Fermi energy lies outside the region of delocalized states then the material is metallic in that the zero-temperature conductivity is non-zero. A metal-insulator transition can be understood to be the consequence of a shift in energy of the mobility edge caused by a decrease in disorder such that in the less disordered samples the Fermi energy is in the region of delocalized states.

A fit was made at low temperatures (up to 50 K) to the dc conductivity by adding a weak-localization correction term appropriate at finite temperature to the interaction term:<sup>13</sup>  $\sigma(T) = \sigma(0) + mT^{1/2} + BT^{p/2}$ , where  $p$  is the exponent for the dominant inelastic scattering process. The fit is good and reproduces the upturn in the HC sample and the downturn in the MC sample, as shown in the inset of Fig. 1. We find  $p = 1.07$  for the HC sample, indicating it is near the metal-insulator transition, and  $p = 2.7$  for the MC sample, indicating a dominating electron-phonon interaction. At temperatures above 50 K, a change in the exponent  $p$  (for example, to  $p = 1$  for conventional electron-phonon scattering) might be expected to lead to changes in temperature dependence. For the LC sample, on the other side of the metal-insulator transition, the conductivity is consistent with hopping behavior,  $\sigma_b(T) = \sigma_h \exp[-(T_h/T)^\gamma]$ , where  $\gamma$  is an indicator of the dimensionality of the conductivity, with which we find  $\gamma = 0.25$  (Fig. 1), suggesting 3D conductivity.

The energy-dependent conductivity [see Fig. 2(b)] has also been fit to the localization-modified Drude (LMD) function,<sup>3</sup>  $\sigma(\omega) = \sigma_D(\omega)[1 - C(1 - l/L)/(k_F)^2]$ , with  $l$  the elastic scattering length and for ac conductivity, the inelastic diffusion length  $L = (D/\omega)^{1/2}$  with the diffusion coefficient  $D = l^2/(3\tau)$ . As can be observed in Fig. 4, if the low fre-

quency molecular vibrationlike peaks are ignored the model captures a number of the experimentally observed features. In particular, it qualitatively reproduces a peak near 0.3 eV, although not the details of its shape, and the temperature dependence is qualitatively accommodated through changes in the scattering rate  $\tau$ . With a decrease in temperature,  $\tau$  increases and the 0.3 eV peak shifts to a lower energy as observed. Furthermore, at low energies ( $\omega < 0.3$  eV) where localization effects dominate, the model predicts a decrease in conductivity with decreasing temperature as observed (Fig. 3). However, as also demonstrated in Fig. 4, the LMD model fails to describe the observed nearly energy-independent conductivity at low energy and instead displays a  $\omega^{1/2}$  dependence.

### III. CONCLUSIONS

Although much of the data in the literature on PF<sub>6</sub>-doped polypyrrole is in general similar, the interpretations presented are quite different. Researchers are divided as to whether the data are best described in terms of homogeneous<sup>2,3</sup> or inhomogeneous microstructure,<sup>4-7</sup> the distinction being in the scale of the disorder. In an effort to distinguish between these two limits, we have analyzed a set of optical measurements made to a high photometric accuracy and have modeled temperature-dependent dc conductivity data on the same samples. By paying attention to the consistency of our derived optical constants, we find no evidence for a large negative dielectric constant at low energy. Moreover, we observe that the low-energy conductivity closely matches the temperature-dependent dc conductivity indicating little evidence for significant spectral weight at lower energies or a significant low-energy coherent electronic conductivity. We find that the two models used to describe the conductivity of PF<sub>6</sub>-doped polypyrrole, the inhomogeneous and homogeneous models, both describe the temperature-dependent dc conductivity and the broad energy-dependent background of the ac conductivity including the temperature dependence and dependence on growth temperature. However, a significant distinguishing feature between the two models is their respective predicted behavior for the low-energy conductivity. With its stronger frequency dependence the LMD model fails to describe the experimentally observed behavior. Therefore, we find that the data can be best described by an inhomogeneous localization model rather than a homogeneous model. However, given the evidence for localization and for inhomogeneity in conducting polymers, the most likely picture is a combination of these two approaches in which the scale and degree of order increases with growth conditions that promote increasing conductivity.

### ACKNOWLEDGMENTS

We wish to thank Ashton Partridge for his help and advice in producing the samples and Tony Bittar for contributing high-energy reflectivity measurements. This work was supported by the New Zealand Foundation for Research, Science and Technology and Victoria University of Wellington.

- <sup>1</sup>*Handbook of Conducting Polymers*, edited by T.A. Skotheim, R.L. Elsenbaumer, and J.R. Reynolds (Marcel Dekker, New York, 1998) pp. 27–121.
- <sup>2</sup>C.O. Yoon, Reghu M., D. Moses, and A.J. Heeger, *Phys. Rev. B* **49**, 10 851 (1994).
- <sup>3</sup>Kwanglee Lee, Reghu Menon, C.O. Yoon, and A.J. Heeger, *Phys. Rev. B* **52**, 4779 (1995); Kwanglee Lee, M. Reghu, E.L. Yuh, N.S. Sariciftci, and A.J. Heeger, *Synth. Met.* **68**, 287 (1995); Kwanglee Lee, Edward K. Miller, Andrei N. Aleshin, Reghu Menon, Alan J. Heeger, Jong Hyun Kim, Chul Oh Yoon, and Hosull Lee, *Adv. Mater.* **10**, 456 (1998).
- <sup>4</sup>R.S. Kohlman, J. Joo, Y.Z. Wang, J.P. Pouget, H. Kaneko, T. Ishiguro, and A.J. Epstein, *Phys. Rev. Lett.* **74**, 773 (1995); R.S. Kohlman, J. Joo, Y.G. Min, A.G. MacDiarmid, and A.J. Epstein, *ibid.* **77**, 2766 (1996); R.S. Kohlman, A. Zibold, D.B. Tanner, G.G. Ihas, T. Ishiguro, Y.G. Min, A.G. MacDiarmid, and A.J. Epstein, *ibid.* **78**, 3915 (1997).
- <sup>5</sup>A.B. Kaiser, *Phys. Rev. B* **40**, 2806 (1989).
- <sup>6</sup>A.B. Kaiser, *Synth. Met.* **45**, 183 (1991).
- <sup>7</sup>L. Zuppiroli, M.N. Bussac, S. Paschen, O. Chauvet, and L. Forro, *Phys. Rev. B* **50**, 5196 (1994).
- <sup>8</sup>F. Wooten, *Optical Properties of Solids* (Academic, New York, 1972).
- <sup>9</sup>A.S. Barker, Jr., *Phys. Rev.* **132**, 1474 (1963).
- <sup>10</sup>Ping Sheng, *Phys. Rev. B* **21**, 2180 (1980).
- <sup>11</sup>R.W. Cochrane and J.O. Strom-Olsen, *Phys. Rev. B* **29**, 1088 (1984).
- <sup>12</sup>N.F. Mott and E.A. Davis, *Electronic Processes in Non-Crystalline Materials* (Clarendon Press, Oxford, 1979), pp. 7–64.
- <sup>13</sup>P.A. Lee and T.V. Ramakrishnan, *Rev. Mod. Phys.* **57**, 287 (1985).